Detection of Thin Films on Polycarbonate and Other Plastic Substrates

Figure 1. The GATR™ Accessory: 65° ATR with Ge crystal.

Figure 2. The FastIR™ Accessory: 45° ATR with ZnSe crystal.

INTRODUCTION

Thin organic coatings or monolayers on semiconductor and metallic substrates are straightforward to detect by FTIR spectroscopy, using either ATR methods[1-5] or grazing angle specular reflectance[6-10]. It is much more difficult to detect such coatings on plastics, because the refractive indices of the two materials are so closely matched. However, detecting these films on plastics, such as polycarbonates, is becoming increasingly important as the industry continues to expand.

Polycarbonates and other plastics are widely used as an alternative for glass in products such as optical lenses, medical devices and electronics equipment. Plastics offer many advantages. They are lighter than glass and do not shatter, in addition to being easy to color, mold and recycle. However, polycarbonates and other plastics weather poorly, scratch easily and are permeable to some gases. To circumvent these limitations, polycarbonate and plastic substrates frequently are coated. These coatings include anti-reflection, anti-abrasion and chemically resistant films. Some of these coatings are extremely thin and not readily detected by standard ATR spectroscopy methods.

This paper explores the use of high incident-angle Ge-ATR to detect these thin coatings on polycarbonates and other plastic substrates.

THEORY

In ATR, the sample must be brought into intimate contact with the optical element, where light is totally internally reflected and the sample interacts with the evanescent wave. This interaction is completely described by the Fresnel equations[1]. These equations

are complex and not particularly insightful. But they do derive the reflectance as a function of the incident angle, incident polarization, and complex refractive indices of the sample and ATR crystal.

In the low absorption limit, the degree of interaction can be measured by an effective pathlength (d_e). This pathlength is defined as the sample thickness which will gives the same absorption as in transmission. For thick films, the effective pathlengths[11] for the two polarizations are:

$$\frac{d_{e\perp}}{\lambda_1} = \frac{n_{21}\cos\theta}{\pi(1-n_{21}^2)(sin^2\theta - n_{21}^2)^{1/2}}$$

$$\frac{d_{e||}}{\lambda_1} = \frac{n_{21}\cos\theta\,(2\sin^2\theta - n_{21}^2)}{\pi(1-n_{21}^2)[(1+n_{21}^2)\sin^2\theta - n_{21}^2](sin^2\theta - n_{21}^2)^{1/2}}$$

where λ_1 is the wavelength, θ is the incident angle, and n_{21} is the refractive index of the sample relative to that of the ATR crystal.

Since the effective thickness is a function of the incident angle and refractive index of the ATR crystal, by using a high refractive index crystal, like Ge, and a high incident angle, it should be possible to distinguish more of the surface characteristics of the sample.

Table 1 shows the effective thicknesses calculated for the GATR™, in comparison to a typical ATR accessory.

	Incident Angle	ATR Crystal	$d_{e\perp}$ (μm)	$d_{e\|\|}$ (μm)
GATR	65°	Ge	0.090	0.168
FastIR	45°	ZnSe	0.205	0.410

Table 1. Differences in Effective Thicknesses at 2000 cm^{-1} for the Two Accessories Used Herein.

EXPERIMENTAL

The ATR spectra were recorded using a Nicolet Nexus 670 spectrometer, configured for data collection at 8 cm^{-1} resolution and 32 scans. The Nexus was equipped with Harrick Scientific Products' GATR™ Thin Film Analyzer (Figure 1) or the FastIR™ (Figure 2) ATR accessories. The GATR™, with its 65° incident angle and Ge ATR crystal, has a lower effective pathlength than traditional horizontal ATR accessories, like the FastIR™, with its 45° incident angle and ZnSe crystal. This gives the GATR™ higher sensitivity to species on the surface of a material.

Background spectra were collected from the clean ATR crystal. Then the samples were compressed against the crystal and the sample spectra collected.

Two different sets of samples were examined: polycarbonate samples and eyeglass lenses. The polycarbonate samples included an uncoated reference and a sample with an unknown coating. The eyeglass lenses were all plastic lenses, possibly also polycarbonates, with an abrasion-resistant coating.

An additional antireflective coating may also have been present on some of the lenses.

RESULTS AND DISCUSSION

The two known polycarbonate samples were examined first to determine if coatings on plastics could be distinguished from the substrate using high incident-angle Ge ATR under ideal circumstances. Figures 3 and 4 show the spectra of the uncoated and coated samples, respectively. Figure 3 is readily identifiable as a polycarbonate, as expected. Figure 4 shows bands that are clearly not from the polycarbonate. In particular, the broad band from 3600 cm^{-1} to 2500 cm^{-1} in the coating does not appear in the substrate and it indicates that the coating is likely to be a carboxylic acid or derivative.

Next, the eyeglass lenses were examined. Since the lens substrates were unknown, spectra were recorded using both the FastIR™ and the GATR™. Since, for the same sample, the GATR™ has a lower effective thickness than the FastIR™ (see Table 1), the GATR™ should sample a greater proportion of the coating relative to the substrate. Comparison of the two spectra should reveal differences between the coating and the substrate.

Figure 5 shows a much narrower band shape for the band around 1100 cm^{-1} in the spectrum recorded with the GATR. In addition, this spectrum shows

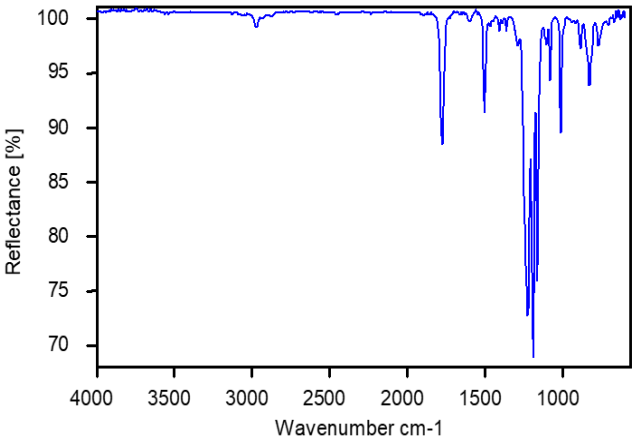

Figure 3. ATR Spectrum of Uncoated Polycarbonate, Recorded with the GATR™.

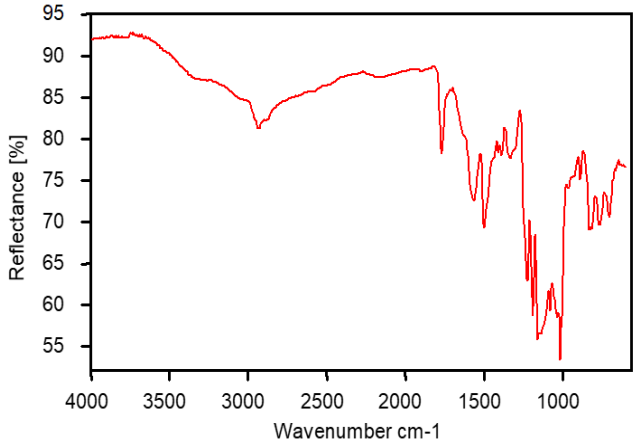

Figure 4. ATR Spectrum of Coated Polycarbonate, Recorded with the GATR™.

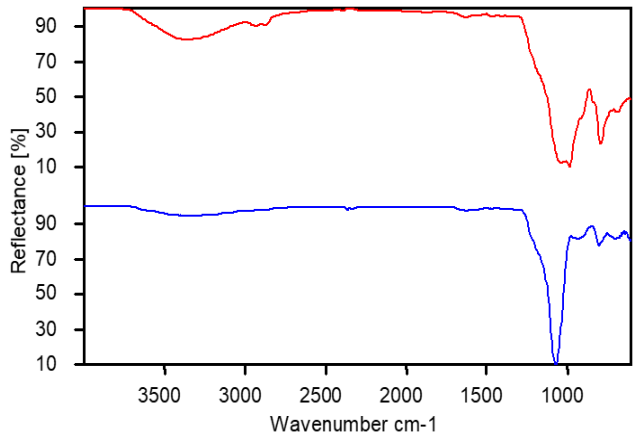

Figure 5. The ATR spectra of Eyeglass Lens A, Recorded with the FastIR™ (top) and GATR™ (bottom).

significantly reduced band intensities in the –OH and –CH region. This would be consistent with a thin metal oxide surface coating. The –OH and –CH bands seen in the spectrum of the lens are probably from the substrate or underlying layer, where their band intensity would be masked by the metal oxide overcoat.

Figures 6 and 7 show spectra from two other lenses. Both Figures show only small differences between the bulk (FastIR) and surface (GATR) spectra, making it more difficult to access whether the differences are due to the coating or to the variations in response between the two sampling methods.

Figure 6 shows a slightly stronger band at 1111 cm^{-1} in the lower spectrum relative to the band at 1020 cm^{-1}. In addition, the bands in the –OH and –CH region are also less intense in the lower spectrum. This may indicate that the band at 1111 cm^{-1} is from the coating and the –OH and –CH bands are in the substrate. The spectra here are similar to that from Figure 5. Both samples are coated with the same material, but the coating is thinner for sample B.

Figure 7 includes spectra from yet a different lens. Here, the lens substrate or under-coating is distinctly different from that shown previously. There is a slight difference in relative band intensities in the fingerprint region for the two spectra recorded, possibly indicating differences in composition between the coating and bulk material.

SUMMARY

With the use of high incident-angle Ge-ATR, thin coatings on polycarbonates and other plastic substrates can be detected. The effectiveness of this method depends on the thickness of the coating. For coatings with thicknesses significantly smaller than the effective thickness, it may be necessary to make measurements at two incident angles, one high and one near critical, to extract information regarding the coating composition. Such measurements could be carried out using a variable angle ATR accessory like the Seagull™.

HARRICK SCIENTIFIC PRODUCTS, INC.
141 Tompkins Avenue, 2nd Floor, PO Box 277
Pleasantville, New York 10570
www.harricksci.com | info@harricksci.com
International: 1-914-747-7202 | USA: 800-248-3847
Fax: 914-747-7209

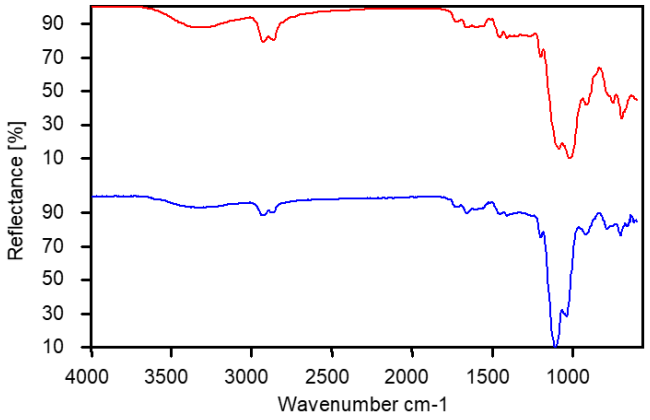

Figure 6. The Normalized ATR spectra of Eyeglass Lens B, Recorded with the FastIR™ (top) and GATR™ (bottom).

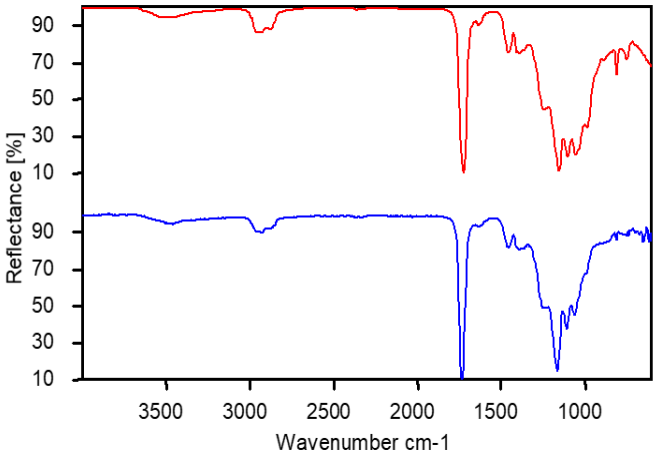

Figure 7. The ATR spectra of an Eyeglass Lens C, Recorded with the FastIR™ (top) and GATR™ (bottom).

ENDNOTES

1. M. Milosevic, S. L. Berets, and Y. Fadeev, *Appl. Spectros.*, 57 (6), 4724 (2003).
2. Mary E. Mulcahy, S. L. Berets, M. Milosevic, and Josef Michl, *J. Phys. Chem. B*, 108 (5), 1519 (2004).
3. Junko Izumitani, Masanori Okuyama and Yoshihiro Hamakawa, *Appl. Spectros.* 47 (9), 1503 (1993).
4. J. E. Olsen and F. Shimura, *J. Appl. Phys.* 65(3), 1353 (1989).
5. J. E. Olsen and F. Shimura, *Appl. Phys. Let.* 53 (20), 1934 (1988).
6. N.J. Harrick and M. Milosevic, *Appl. Spectros.* 44 (3), 519 (1990).
7. S. A. Francis and A. H. Ellison, *J. Opt. Soc. Am.* 49 (2), 131 (1959).
8. Richard M. Crooks, Chuanjing Xu, et. al., *Spectros.* 8(7), 28 (1993).
9. E. I. Firsov and P. A. Shafranovsky, *Surf. Sci. Let.* 244, 113 (1991).
10. D. L. Allara, A. Baca, and C.A. Pryde, *Macromol.* 11 (6), 1215 (1978).
11. N.J. Harrick, *Internal Reflection Spectroscopy* (John Wiley and Sons, Inc., 1967).
12. M. Milosevic and S. L. Berets, *Appl. Spectros.* 47 (5), 566 (1993).
13. Using Harrick Scientific's CristalCalc™.